
Proceedings Paper:
Hoang, K.D., Wang, J., Cyriacks, M. et al. (2013) Feed-forward Torque Control of Interior Permanent Magnet Brushless AC Drive for Traction Applications. In: Electric Machines & Drives Conference (IEMDC), IEEE International. 2013 IEEE International Electric Machines & Drives Conference, 12-15 May 2013, Chicago, Illinois. IEEE, pp. 152-159. ISBN: 978-1-4673-4975-8.

https://doi.org/10.1109/IEMDC.2013.6556247

Feed-forward Torque Control of Interior Permanent Magnet Brushless AC Drive for Traction Applications

K. D. Hoang, *Member, IEEE*, J. Wang, *Senior Member, IEEE*, M. Cyriacks, A. Melkonyan, and K. Kriegel

***Abstract*—This paper presents a feed-forward torque control (FTC) technique for interior permanent magnet (IPM) brushless AC (BLAC) drives in traction applications. It is shown that by adopting the Newton-Raphson iterative method for solving the proposed high-order nonlinear relationship between the torque demand, flux-linkage and desirable *dq*-axis currents, FTC with due account of nonlinear machine parameters can be achieved for IPM BLAC drives. It is also proven that the comparison between the reference voltage magnitudes under maximum torque per ampere (MTPA) and field-weakening (FW) operations together with online base speed determination can be utilized for FW operation activation to achieve full exploitation of the available DC-link voltage during the transition between the constant torque and FW operation regions. Since both the *dq*-axis current references and the base speed for FW operation activation are computed online, the proposed FTC technique provides flexibility for online parameter update or estimation and is able to cope with wide DC-link voltage variation. The proposed FTC strategy is experimentally validated by measurements on a 10kW wide constant power speed range (CPSR) IPM BLAC machine drive.**

***Index Terms*— Feed-forward torque control (FTC), field weakening (FW) operation, interior permanent magnet (IPM) brushless AC (BLAC) machine, maximum torque per ampere (MTPA) operation.**

I. Introduction

Due to high efficiency and wide field weakening capability, interior permanent magnet (IPM) brushless AC (BLAC) machine is often employed in traction applications [1], [2]. However, an IPM BLAC machine is well-known for its nonlinear machine parameters owning to saturation and cross-coupling effects [3] which affect the quality of torque control. Thus, these effects have to be taken into consideration for high performance operation. In a traction application employing IPM BLAC machine, torque control is generally required. Therefore, an effective torque control strategy for a full speed operating range is essential. It should give the drive system the flexibility of online parameter estimation/adaptation [4-5] and ability to accommodate DC-link or battery voltage variation.

To date, a great number of control schemes were proposed for IPM BLAC drives [1], [2], [6], [7], and [8]. However, all these studies were focused on the speed control where the output of the speed controller is not the torque demand, but signals proportional to the *q*-axis current [1-2], the *q*-axis current demand [6], or the phase current amplitude [7-8]. This will inevitably introduce nonlinearity into the control loop. On the other hand, the *d*-axis current demand under these proposed control schemes is generated based on the assumption that the machine parameters are constant. Actually, this is not true for most IPM machines [3].

Torque control methodologies for IPM BLAC drives with voltage feedback (VFB)-based stator flux reference regulation were reported in [9], [10], and [11] where the *d*- and *q*- axis current demands are obtained from predefined look-up tables (LUT) with torque and flux-linkage magnitude as their inputs. As these LUTs are defined offline based on the nonlinear machine model, it is difficult to accommodate parameter variation during operation, such as temperature effect and large variation of the DC-link voltage. In [10], it was demonstrated that the VFB-based torque control scheme presented in [9] cannot make full use of the available DC-link voltage due to the conflict between the anti-windup and the current regulators. The transition between the constant torque and the field weakening (FW) regions under the proposed VFB-based torque control scheme in [10] depends on the VFB gain and the base speed of the IPM BLAC machine. It is noted that the base speed significantly depends on the nonlinear machine parameters, the DC-link voltage, and the employed modulation technique. Consequently, excessive *d*-axis current may result and compromise drive efficiency. Similar issues can be found in [11] where a predefined steady state modulation index reference which is computed offline based on the nonlinear machine paramaters together with VFB controller were utilized to activate and maintain the FW operation.

In this paper, the mathematical descriptions representing the

This work was supported in part by the European Commission under Grant No. 260087.

K. D. Hoang and J. Wang are with the Department of Electronic and Electrical Engineering, The University of Sheffield, Sheffield, United Kingdom (e-mail: k.hoang@sheffield.ac.uk; j.b.wang@sheffield.ac.uk).

M. Cyriacks, A. Melkonyan, and K. Kriegel are with Siemens AG, CT RTC POA POE-DE, Otto-Hahn-Ring 6, 81739 München, Deutschland (email:marco.cyriacks@siemens.com;ashot.melkonyan@siemens.com; kai.kriegel@siemens.com).

relationship between the torque demand, the flux linkage and the desired *dq*-axis current components for feed-forward torque control (FTC) under maximum torque per ampere (MTPA) operation and field weakening (FW) operation are introduced. Since for a given torque and speed, the governing equation for *dq*-axis currents are 4th order polynomial, it is shown that good accuracy for solving *d*- and *q*- axis current references can be achieved by employing the Newton-Raphson iterative method [12] and selecting appropriate initial values. It is also demonstrated that the comparison between the reference voltage magnitudes under MTPA and FW operations together with online base speed determination can be employed for FW operation activation to make full use of the available DC-link voltage during the transition between the constant torque and FW operating modes. Since the base speed for FW operation activation and the *dq*-axis current references for a given torque demand and speed are computed online under the proposed FTC technique, it provides flexibility for online parameter update or estimation and facilitate full use of available DC-link voltage which could vary considerably.

This paper is organized as follows. In Section II, the mathematical model of IPM BLAC machine together with its current and voltage limiting trajectories in the rotational (*dq*) reference frame is presented. The proposed FTC technique for IPM BLAC drive with suitable transition between the MTPA and the FW operating regions is described in Section III. In Section IV, measured results are reported to experimentally validate the proposed FTC methodology.

II. Mathematical Model for Optimal Operation of IPM BLAC Machine

A. Mathematical model of IPM BLAC machine

The mathematical model of an IPM BLAC machine in the (*dq*) reference frame can be expressed as follows [1, 2]:

$$v_d = R_s i_d - \omega_e \psi_{sq} + \frac{d\psi_{sd}}{dt} \tag{1}$$

$$v_q = R_s i_q + \omega_e \psi_{sd} + \frac{d\psi_{sq}}{dt} \tag{2}$$

$$\psi_{sd} = L_d i_d + \psi_m \tag{3}$$

$$\psi_{sq} = L_q i_q \tag{4}$$

$$T_e = \frac{3}{2} p i_q [\psi_m + (L_d - L_q) i_d] \tag{5}$$

where $v_{d,q}$, $i_{d,q}$, $\psi_{sd,sq}$, $L_{d,q}$ are the transformed (*dq*) voltages, currents, stator flux-linkages, and stator inductances, respectively; ω_e is the electrical rotor speed; R_s is the stator resistance; ψ_m is the flux linkage due to PM field; T_e is the electromagnetic torque and *p* is the pole-pair number.

B. Current and voltage limits of IPM BLAC machine drive

1) Current limit circle

The current limit of a drive system depends on both the current rating of the machine and inverter. Normally, maximum operating current of the drive system should be kept below a maximum permissible value, I_m. Thus, the current limit circle can be defined as

$$i_d^2 + i_q^2 \le I_m^2 \tag{6}$$

2) Voltage limit ellipse

In a drive system, the maximum available fundamental phase voltage depends on modulation technique and supply DC-link voltage [13]. Since the time derivations in (1) and (2) are zero in steady state, the voltage limitation associated with the induced voltage [6], v_{d0} and v_{q0}, can be expressed as:

$$\sqrt{v_{d0}^2 + v_{q0}^2} = V_0 \le V_{0m} = k_M V_{dc} - R_s I_m \tag{7}$$

$$v_{d0} = -\omega_e L_q i_q \,;\, v_{q0} = \omega_e (L_d i_d + \psi_m) \tag{8}$$

where V_{dc} is the DC-link voltage; V_{0m} is the equivalent maximum induced voltage; and k_M is the modulation factor associated with an modulation technique [13] as shown in Table I. Fig. 1(a) presents the current and voltage constraints of the IPM BLAC machine employed in this study. It is worth noting that when the operating speed is higher than the machine base speed (ω_{base}), the maximum achievable torque at a given speed for the IPM BLAC machine is determined via the intersections between the voltage and current constraints.

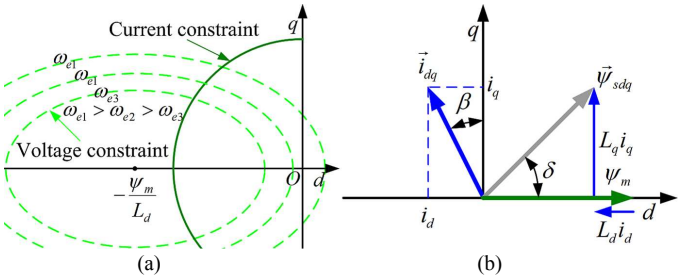

Fig. 1. Performance of IPM BLAC drives. (a) Operating limitations. (b) Current and stator flux vector diagrams.

TABLE I
MODULATION FACTOR k_M ASSOCIATED WITH DIFFERENT MODULATION TECHNIQUES [13]

Sinusoidal PWM (SPWM)	Third-harmonic injection PWM (THIPWM)	Space-vector PWM (SVM)	Six-step PWM
$\frac{1}{2}$	$\frac{1}{\sqrt{3}}$	$\frac{1}{\sqrt{3}}$	$\frac{2}{\pi}$

III. Proposed FTC Strategy For IPM Machine Considering Nonlinear Parameters

A. Proposed FTC technique for Maximum Torque per Ampere (MTPA) Operation

From Fig. 1, without the voltage limit, *dq*-axis current

components can be expressed as

$$i_d = -\left|\vec{i}_{dq}\right|\sin(\beta)\ ;\ i_q = \left|\vec{i}_{dq}\right|\cos(\beta) \tag{9}$$

where $\left|\vec{i}_{dq}\right| = I_{mag} = \sqrt{i_d^2 + i_q^2}$ is the magnitude of the stator phase current vector. Substituting (9) into (5) gives

$$T_e = \frac{3}{2}p[\psi_m I_{mag}\cos(\beta) + (L_q - L_d)I_{mag}^2\sin(\beta)\cos(\beta)] \tag{10}$$

According to [12], for a given current magnitude, the optimal angle β for maximum torque can be obtained by solving (11)

$$\frac{dT_e}{d\beta} = \frac{3}{2}p[-\psi_m I_{mag}\sin(\beta) + (L_q - L_d)I_{mag}^2\cos(2\beta)] = 0 \tag{11}$$

which yields

$$\sin(\beta) = \frac{-\psi_m + \sqrt{\psi_m^2 + 8I_{mag}^2(L_q - L_d)^2}}{4(L_q - L_d)I_{mag}} \tag{12}$$

Substituting (12) into (9) and solving for the *d*-axis current yields (13) for the MPTA operation

$$i_d = \frac{\psi_m}{2(L_q - L_d)} - \sqrt{\frac{\psi_m^2}{4(L_q - L_d)^2} + i_q^2} \tag{13}$$

Substituting (13) into the torque equation (5) leads to

$$f_{MTPA}(i_q) = (L_d - L_q)^2 i_q^4 + \frac{2T_e}{3p}\psi_m i_q - \left(\frac{2T_e}{3p}\right)^2 = 0 \tag{14}$$

Equation (14) presents the mathematical relationship between the demanded torque and the required *q*-axis current to achieve the MTPA operation in the constant torque operation region. Illustration of MTPA operation trajectory for IPM BLAC machine is presented in Fig. 2 (OABCD trajectory). Since (14) is a 4th-order polynomial, the Newton-Raphson iterative method [12] may be employed as follows.

$$i_{qMTPA}(k+1) = i_{qMTPA}(k) - \frac{f_{MTPA}(i_{qMTPA}(k))}{f'_{MTPA}(i_{qMTPA}(k))} \tag{15}$$

$$f'_{MTPA}(i_q) = 4(L_d - L_q)^2 i_q^3 + \frac{2T_e}{3p}\psi_m \tag{16}$$

where $f'_{MTPA}(\cdot)$ denoted the derivative of $f_{MTPA}(\cdot)$ and $i_{qMTPA}(k)$ is the k^{th} iteration of the *q*-axis current demand for the proposed FTC technique with MTPA operation, i_{qMTPA}. To ensure rapid convergence, selection of suitable initial root values is

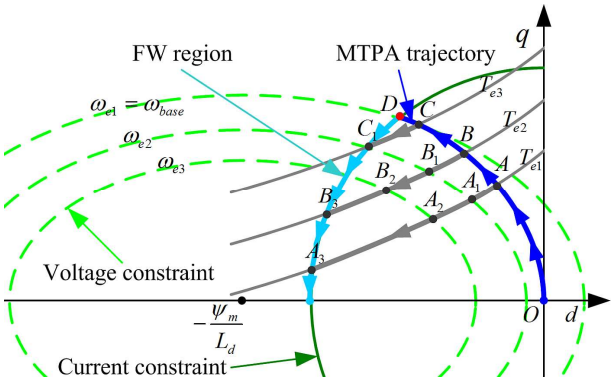

Fig. 2. Optimal operation of IPM BLAC machine under constant torque operation region and FW region.

essential. The initial root value of (15) can be obtained by neglecting the 4th order term of (14) and solving

$$i_{qMTPA}(0) = \frac{2T_e}{3p\psi_m} \tag{17}$$

Normally, a convergence condition, ξ, should be defined for the iterative process

$$\Delta i_{qMTPA}(k+1) = i_{qMTPA}(k+1) - i_{qMTPA}(k) < \xi \tag{18}$$

where ξ is often chosen based on decimal places of the expected approximation accuracy. The implementation of the Newton-Raphson iterative method for the proposed FTC technique with MTPA operation is illustrated in Fig. 3(a). However, it is worth noting that the sampling interval in a DSP-based drive system is fixed. Therefore, there is a trade-off between the number of iterations for high approximation accuracy and the required computation time. Normally, the number of iteration should be limited when sufficient accuracy has been reached. Fig. 3(b) shows that good accuracy up to 3 decimal places (1-9mA error, i.e., 0.001-0.009% of the actual *q*-axis current value) can be achieved after only 4 iterations for the IPM BLAC machine with a step change 20Nm of torque demand at 1000rpm. Once (14) has been solved, the *d*-axis current demand for the proposed FTC technique with MTPA operation, i_{dMTPA}, can be derived from the torque equation (5) as follows:

$$i_{dMTPA} = \frac{2T_e}{3pi_{qMTPA}(L_d - L_q)} - \frac{\psi_m}{(L_d - L_q)} \tag{19}$$

.

B. Base speed of IPM BLAC machine

For an IPM BLAC machine, its base speed is defined by the intersection between the MTPA trajectory, the current limit circle, and the voltage limit ellipse (point D in Fig. 2) [7]. By substituting (6) into (13) and solving, the *d*-axis current at the intersection point D (i_{dBASE}) can be derived as

$$i_{dBASE} = \frac{\psi_m - \sqrt{\psi_m^2 + 8(L_q - L_d)^2 I_m^2}}{4(L_q - L_d)} \tag{20}$$

Since the intersection point D is located in the voltage limit ellipse associated with the base speed, substituting (6) and (20) into (7) and solving yields the base speed for FW control activation as

$$\omega_{base} = \frac{V_{0m}}{\sqrt{(L_d i_{dBASE} + \psi_m)^2 + L_q^2 (I_m^2 - i_{dBASE}^2)}} \tag{21}$$

As can be seen from (21), the base speed value depends on the machine parameters, the maximum operating current, the supply DC-link voltage, and the selected modulation technique. Fig. 4(d) illustrates the base speed variation of the IPM BLAC machine with the DC-link (battery) voltage variation. In practice, this value is essential for FW control activation of IPM BLAC machine, [6] and [10].

C. Proposed FTC technique for Field Weakening (FW) Operation

When the operating speed of the IPM BLAC drive is higher than its base speed, the *dq*-axis current references must be selected to maintain both the torque demand and the voltage boundary. From Fig. 2, it can be seen that for a given torque demand T_{e1}, the operating point should be A_1 for the speed of ω_{e2} and A_2 for ω_{e3}. The operating point for a given torque demand and speed in the FW operation region can be obtained by substituting (5) into (7) and solving (22) for the *d*-axis current demand of the proposed FTC technique with FW operation (i_{dFW})

$$f_{FW}(i_d) = a_4 i_d^4 + a_3 i_d^3 + a_2 i_d^2 + a_1 i_d + a_0 = 0 \tag{22}$$

where

$$\begin{cases} a_0 = -\psi_m^2 B + \left(\dfrac{2T_e}{3p} L_q\right)^2; a_1 = 2L_d \psi_m^3 - 2AB\psi_m \\ a_2 = L_d^2 \psi_m^2 + 4L_d \psi_m^2 A - BA^2; a_3 = 2L_d \psi_m A^2 + 2A\psi_m L_d^2 \\ a_4 = L_d^2 A^2; A = L_d - L_q; B = \left(\dfrac{V_{0m}}{\omega_e}\right)^2 - \psi_m^2 \end{cases}$$

It is worth noting that value of V_{0m} depends on the modulation factor k_M as shown in Table I. Therefore, for an IPM BLAC drive system with overmodulation (OM) technique [14], a selection of $k_M = 2/\pi$ may make full use of the available DC-link voltage. As (22) is also a 4th order polynomial, the Newton-Raphson iterative method (15) should be utilized for implementation of the proposed FTC technique with the FW operation. The derivative of (22) for the Newton-Raphson approximation can be expressed as

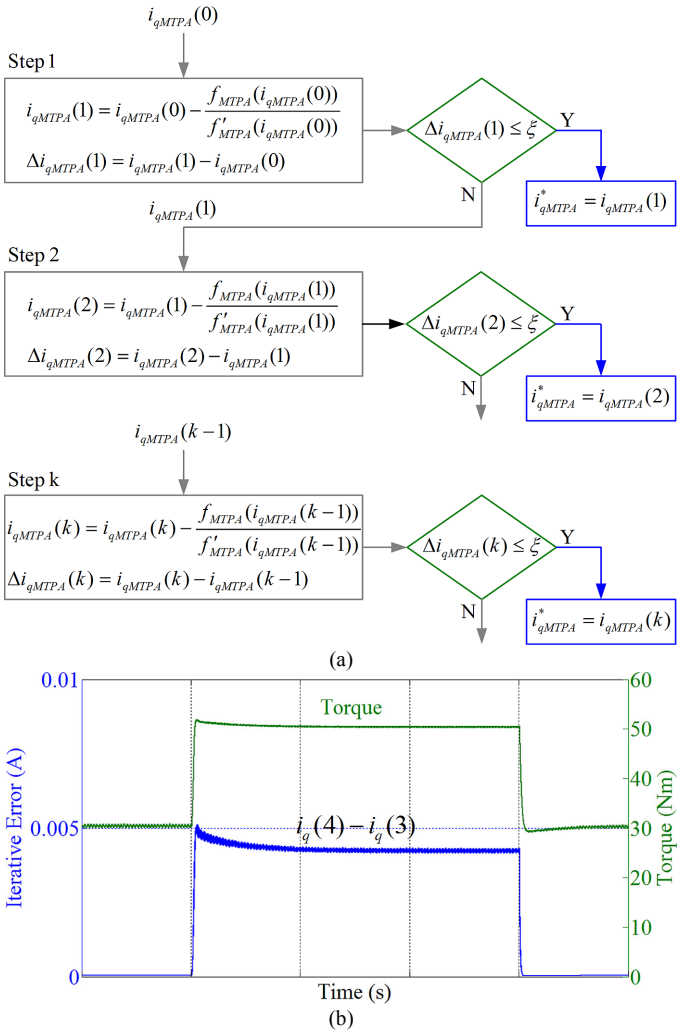

Fig. 3. Newton-Raphson iteration for solving proposed FTC technique with MTPA operation. (a) Block diagram. (b) Iterative error for a step change 20Nm of torque demand at 1000rpm.

$$f'_{FW}(i_d) = 4a_4 i_d^3 + 3a_3 i_d^2 + 2a_2 i_d + a_1 \tag{23}$$

The initial root value for approximation of (22) can be derived by neglecting the 3rd and 4th order terms and solving

$$i_{dFW}(0) = \frac{-a_1 + \sqrt{a_1^2 - 4a_2 a_0}}{2a_2} \tag{24}$$

After (22) has been solved, the *q*-axis current demand for the proposed FTC technique with FW operation can be derived from the torque equation (5) and is given by:

$$i_{qFW} = \frac{2T_e}{3p[\psi_m + (L_d - L_q) i_{dFW}]} \tag{25}$$

From (14) and (22), it is obvious that under the proposed FTC technique, the *dq*-axis current references associated with the torque demand at a given speed are computed online for both constant torque and FW operation regions. Therefore, it provides flexibility for online parameter update or estimation

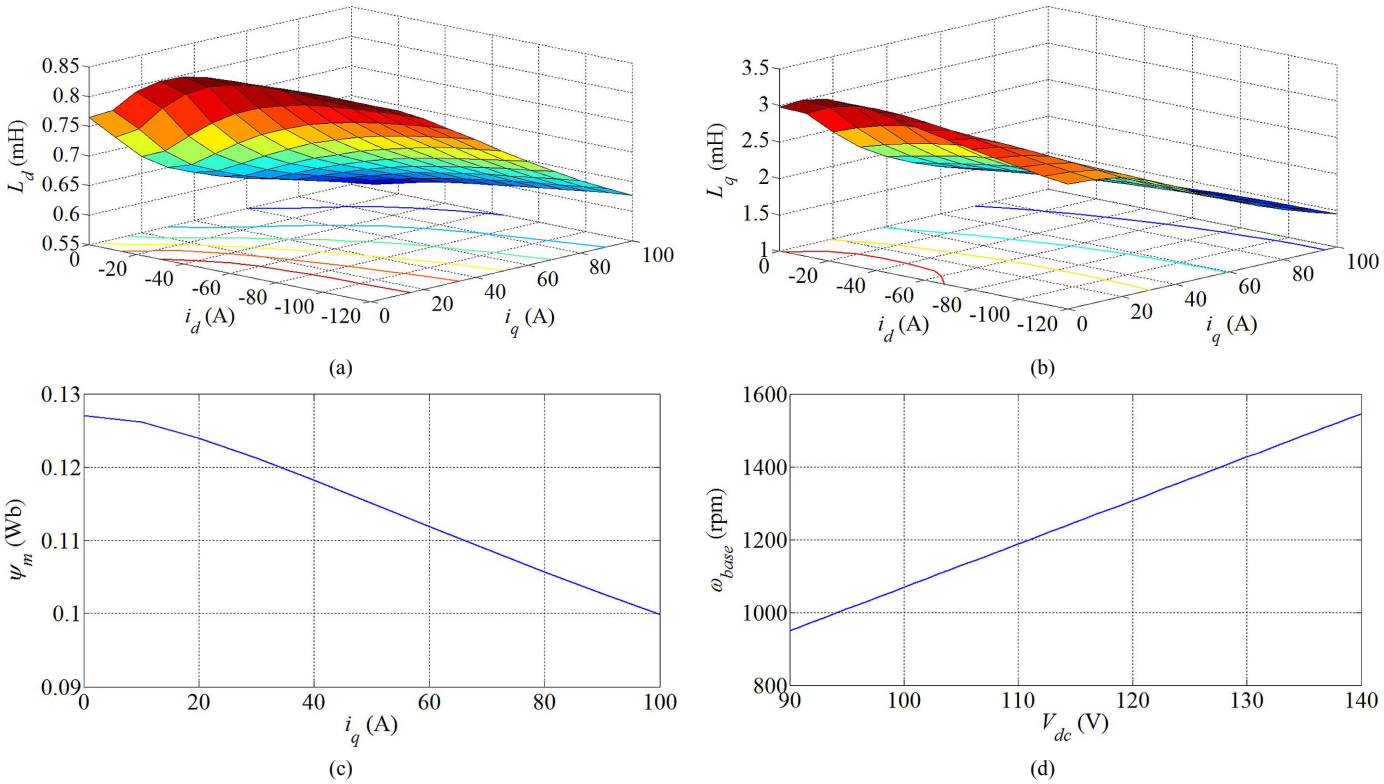

Fig. 4. Nonlinear IPM BLAC machine parameters. (a) L_d as a function of *dq*-axis currents. (b) L_q as a function of *dq*-axis currents. (c) ψ_m as a function of *q*-axis current. (d) ω_{base} as a function of nonlinear IPM BLAC machine parameters and DC-link voltage variation.

and ability to cope with wide DC-link voltage variation and to make full use of available battery voltage.

D. Nonlinear Parameter Issue of IPM BLAC Machine

To implement the proposed FTC technique, the machine parameters for computing relevant *dq*-axis current references from a torque demand value must be available. However, the parameters of IPM BLAC machines are often nonlinear and defined as functions of *d*- and *q*- axis currents [3], [10], [11], and [15]. The nonlinear machine parameters of the IPM BLAC machine employed in this study are illustrated in Fig. 4. It is worth noting that these nonlinear parameters can be obtained using the measurement technique proposed in [15].

E. Transition scheme between the MTPA and FW operations for the proposed FTC technique

In [6], based on the assumption that the induced voltage magnitude [obtain by solving (7)] under FW operation (V_{0FW}^*) are equal to the equivalent maximum induced voltage V_{0m}, it was suggested that FW operation can be activated by comparing between V_{0m} and the induced voltage reference magnitude under MTPA operation (V_{0MTPA}^*) [Fig. 5(a)]. In practice, V_{0m} and V_{0FW}^* may not always be equal. Thus, under this scheme, full exploitation of the available DC-link voltage may not be achieved. On the other hand, effects of stator resistance voltage drop are also neglected. In this paper, to fully exploit the available DC-link voltage and take into account the stator resistance voltage drop, voltage reference magnitudes [obtain by solving (1) and (2)] under MTPA (V_{MTPA}^*) and FW (V_{FW}^*) operations is compared as shown in Fig. 5(b) to activate FW operation. Also from Fig. 5(b), it is noted that implementation of the modified FW transition scheme requires prior knowledge of the base speed. In an IPM BLAC drive for traction application with nonlinear machine parameters (Fig. 4) and variable DC-link (battery) voltage, the base speed is not fixed. A lower base speed than the actual one may trigger earlier FW operation, which results in not making full use of the available DC-link voltage and hence lower efficiency. Besides, a higher base speed than the actual one may cause voltage saturation in the drive system with unexpected torque reduction at high-speed operations. Thus, for the proposed FTC technique to achieve maximum output torque under a given DC-link voltage in both MTPA and FW operating modes, the base speed should be determined online using (21). The modified FW transition scheme illustrated in Fig. 5(b) is as follows:

1) If the operating speed is lower than the base speed (ω_{e1} in Fig. 2), the MTPA operation is selected and operating point associated with a given torque demand follows the MTPA trajectory (OABCD) as shown in Fig. 2.
2) When the operating speed (ω_{e2} in Fig. 2) is higher than the base speed, for a given torque demand (T_{e2} in Fig. 2), the operating point is chosen between B and B_1 based on the comparison between V_{MTPA}^*

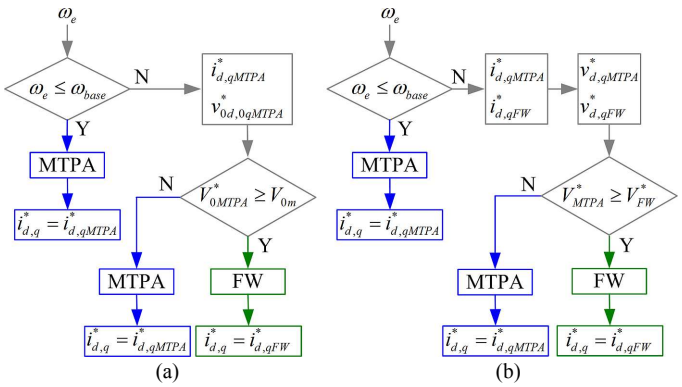

Fig. 5. FW transition schemes between MTPA and FW operations for proposed FTC technique. (a) Conventional scheme [6]. (b) Modified scheme.

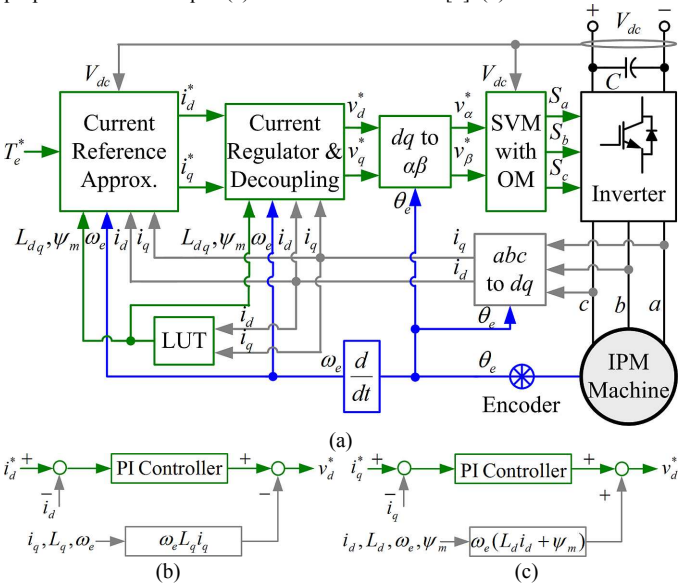

Fig. 6. Proposed FTC IPM BLAC drive. (a) Block diagram. (b) D-axis current regulator and decoupling: $K_{Pd} = L_d\omega_c$; $K_{Id} = R_s\omega_c$ [4]. (c) Q-axis current regulator and decoupling: $K_{Pq} = L_q\omega_c$; $K_{Iq} = R_s\omega_c$ [4].

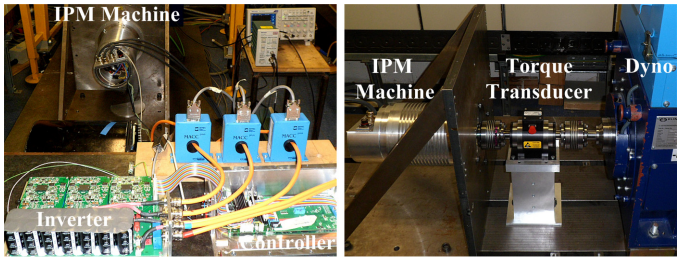

Fig. 7. Experimental hardware setup. (a) Inverter and DSP-based control platform. (b) IPM BLAC machine coupled to dynamometer via torque transducer.

and V^*_{FW} , Fig. 5(b). Since the base speed is computed online using the machine nonlinear parameters and the DC-link voltage measurement as shown in (21), the variation of the DC-link voltage and machine parameters can be taken into account.

The block diagram of the proposed FTC technique is presented in Fig. 6 where the superscript "*" indicates the reference values. To provide the instantaneous machine parameters for the IPM BLAC drive, three predefined LUTs

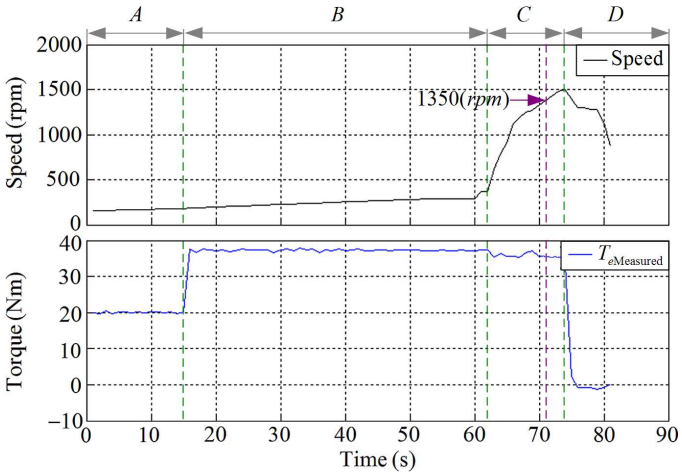

Fig. 8. Steady state and dynamic test of proposed FTC technique for IPM BLAC drive under MTPA operation. A: Slowly acceleration with 20Nm torque demand. B: Slowly acceleration with 15Nm step change on torque demand. C: Acceleration from 400rpm to 1500rpm with 35Nm continuous torque demand. D: Deceleration with zero torque demand.

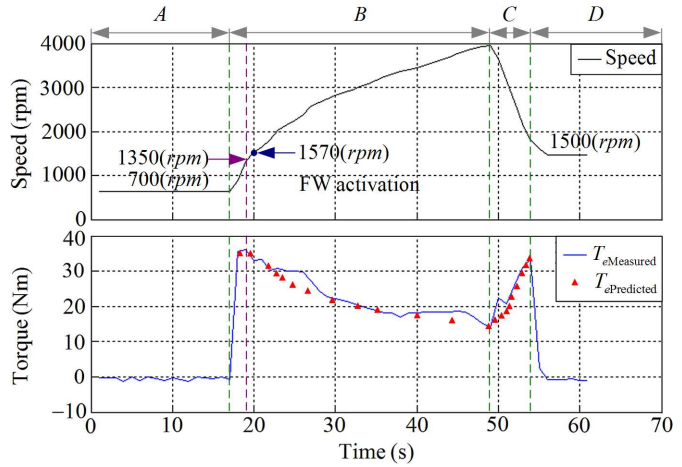

Fig. 9. Dynamic test of proposed FTC technique for IPM BLAC drive under FW operation. A: Constant speed with zero torque demand. B: Acceleration up to 4000rpm with 35Nm continuous torque demand. C: Deceleration with 35Nm continuous torque demand. D: Deceleration down to 1500rpm with zero torque demand.

TABLE II
IPM BLAC MACHINE PARAMETERS

Number of pole-pairs	3
Phase resistance	51.2 (mΩ)
Continuous/maximum current	58.5/118 (A)
Peak power below based speed	10 (kW)
DC link voltage	120(V)
Based/maximum speed	1350/4500 (rpm)
Continuous/peak torque	35.5/70 (Nm)
Peak power at maximum speed	7 (kW)

based on Figs. 4(a), 4(b) and 4(c) are employed. First, the base speed is computed via (21). Then, operation mode will be decided using the selection scheme shown in Fig. 5(b). The current references for a given torque demand are computed using the aforementioned FTC technique. The cutoff frequency of the two PI current controllers (ω_c) shown in

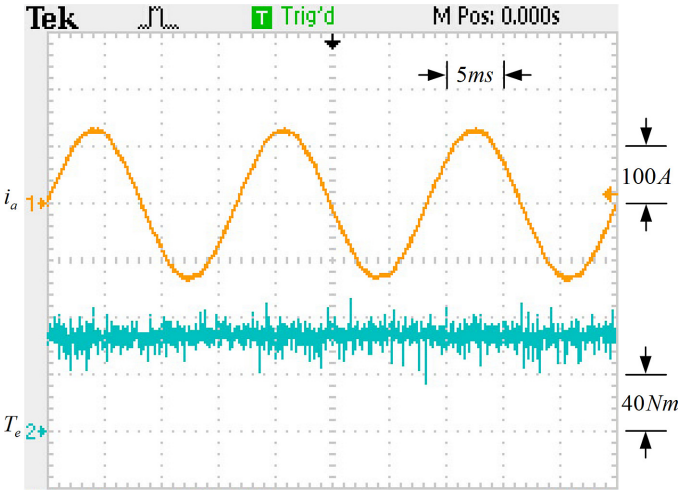

(a)

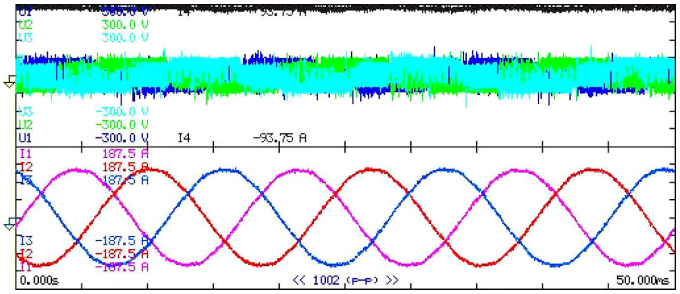

(b)

Fig. 10. Measured results of proposed FTC for IPM BLAC drive under MTPA operation at 1200rpm, 70Nm peak torque demand. (a) Phase *a* current and torque waveforms. (b) 3-phase current and voltage waveforms.

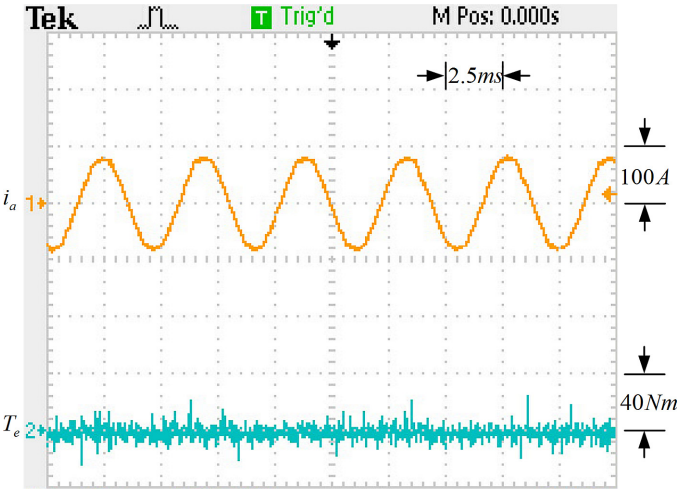

(a)

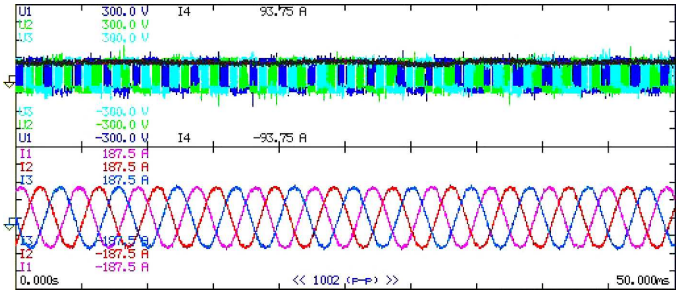

(b)

Fig. 11. Measured results of proposed FTC for IPM BLAC drive under FW operation at 4500rpm, 5Nm torque demand. (a) Phase *a* current and torque waveforms. (b) 3-phase current and voltage waveforms.

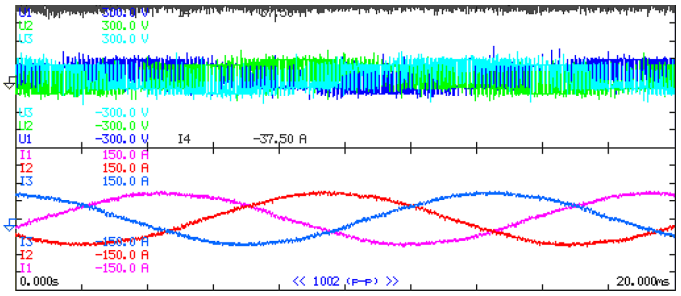

(a)

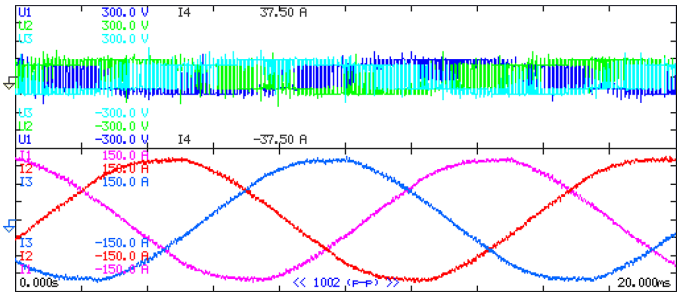

(b)

Fig. 12. Measured results of proposed FTC technique under MTPA operation at base speed (1350rpm). (a) 35Nm continuous torque demand. (b) 70Nm peak torque demand

Figs. 6(b) and 6(c) is chosen as 5 to 10 times of the maximum operating frequency of the IPM BLAC machine, Table II.

IV. Experimental Results

To demonstrate the proposed FTC technique, a test-rig with a 10kW wide CPSR (3.333) IPM BLAC machine designed for traction application has been set up as shown in Fig. 7. The machine exhibits nonlinear parameters (Fig. 4) and its ratings are provided in Table II. It is worth noting that the overmodulation technique presented in [14] is utilized together with the modulation factor $k_M = 2/\pi$ to exploit the available DC-link voltage under the proposed FTC technique. A voltage transducer is utilized to track the DC-link voltage variation. The switching frequency is set as 8(kHz) and a magnetic encoder (Renishaw RM44SC0011B20F2F10) is employed to provide the rotor position information for the controller. A precision power analyzer (Yokogawa WT3000) together with an in-line torque transducer is used to measure currents, voltage, and efficiency of the inverter and the IPM BLAC machine.

To validate the proposed FTC technique, dynamic tests under both constant torque and FW operation region were respectively performed, Figs. 8 and 9. During the tests, the drive operated in torque control mode and its speed was controlled by the dynamometer. Fig. 8 shows the speed and torque variations of the drive operating in the constant torque operation region with the proposed FTC technique. As can be

seen, good torque control is maintained regardless of the speed variation and a 15Nm step change in torque demand. The torque response to the step changes is smooth with virtually no overshooting. It is noted that MTPA operation is still maintained for the tested IPM BLAC drive when the operating speed is higher than the base speed (1350rpm) with 35Nm continuous torque demand under the modified FW transition scheme shown in Fig. 5(b). Since the MTPA operation is selected for the operating points from 1350rpm to 1500rpm with 35Nm continuous torque demand due to their lower voltage reference magnitudes compared with that of the FW operation, the available DC-link voltage is fully exploited with the proposed FTC technique.

The results obtained from dynamic test of the proposed FTC technique in the FW operation region is presented in Fig. 9. It is shown that the generated torque of the IPM BLAC drive, when the speed was increased from 700rpm to 4000rpm and decreased from 4000rpm to 1500rpm, follows the maximum power boundary ($DC_1B_3A_3$) shown in Fig. 2. The measured torque variation matches well with the predicted results for both acceleration and deceleration tests. A smooth transition from the constant torque to the FW operation regions when the operating speed approaches 1570rpm under 35Nm continuous torque demand can be observed at t = 20(s).

Measured results with 3-phase balanced sinusoidal current waveforms and smooth torque production in the steady state at 1200rpm and 70Nm (MTPA operation, maximum power) and at 4500rpm and 5Nm (FW operation, maximum speed) are shown, respectively, in Figs. 10 and 11 to validate the proposed FTC technique incorporating the nonlinear machine parameters for wide CPSR IPM BLAC machine. In addition, to express the efficiency of the modified FW transition scheme with online base speed determination, voltage and current waveforms of the tested IPM BLAC machine under the proposed FTC technique at 1350rpm (base speed) are presented in Fig. 12(a) for 35Nm continuous torque demand and Fig. 12(b) for 70Nm peak torque demand, respectively. Since the voltage limit of the drive system reaches the hexagon boundary [14] at the base speed under peak torque demand, the available DC-link voltage at this operating point is fully exploited. Thus, compared with Fig. 12(a), 3-phase flat-top current waveforms can be observed from Fig. 12(b).

It is worth noting that measured results from Figs. 8 to 12 with good overall dynamic response, smooth transition between the constant torque and the FW operating regions with full DC-link voltage exploitation, together with 3-phase balanced sinusoidal current waveforms and smooth torque production in the steady state are experimentally verified the proposed FTC technique incorporating the nonlinear machine parameters using the Newton-Raphson iterative method.

V. Conclusion

In this paper, a feed-forward torque control strategy incorporating nonlinear machine parameters for a wide CPSR IPM BLAC drive in traction applications has been described and experimentally validated. Since the relationship between the torque demand and *dq*-axis current components are governed by 4th order polynomials in both constant torque and field weakening regions, it has been shown that good accuracy for *d*- and *q*- axis current references can be achieved by employing the Newton-Raphson iterative method and selecting appropriate initial root values.

It has been demonstrated that the comparison between the reference voltage magnitudes under MTPA and FW operations together with online base speed determination can be employed for FW operation activation to make full use of the available DC-link voltage during the transition between the constant torque and FW operation regions. The proposed FTC technique can be easily incorporated with online parameter update to improve torque control accuracy and drive efficiency, and has the ability to cope with wide DC-link voltage variation.

References

[1] C. T. Pan and S. M. Sue, "A linear maximum torque per ampere control for IPMSM drives over full-speed range," *IEEE Trans. Energy Conver.,* vol. 20, no. 2, pp. 359-366, Jun. 2005.

[2] S. M. Sue and C. T. Pan, "Voltage-constraint-tracking-based field-weakening control of IPM synchronous motor drives," *IEEE Trans. Ind. Electron.*, vol. 55, no. 1, pp. 340-347, Jan. 2008.

[3] B. Stumberger, G. Stumberger, D. Dolinar, A. Hamler, and M. Trlep, "Evaluation of saturation and cross-magnetization effects in interior permanent magnet synchronous motor," *IEEE Trans. Ind. App.*, vol. 39, no. 5, pp. 1264-1271, Sep./Oct. 2003.

[4] Y. A. I. Mohamed and T. K. Lee, "Adaptive self-turning MTPA vector controller for IPMSM drive system," *IEEE Trans. Energy Convers.*, vol. 21, no. 3, pp. 636-644, Sep. 2006.

[5] H. Kim, J. Hartwig, and R. D. Lorenz, "Using on-line parameter estimation to improve efficiency of IPM machine drives," in *Proc. IEEE Power. Electron. Spec. Conf.*, 2002, pp. 815-820.

[6] S. Morimotor, M. Sanada, and Y. Takeda, "Effect and compensation of magnetic saturation in flux-weakening controlled permanent magnet synchronous motor drives," *IEEE Trans. Ind. Appl.*, vol. 30, no. 6, pp. 16320-1637, Nov./Dec. 1994.

[7] J. M. Kim and S. K. Sul, "Speed control of interior permanent magnet synchronous motor drive for the flux-weakening operation," *IEEE Trans. Ind. Appl.*, vol. 33, no. 1, pp. 43–48, Jan./Feb. 1997.

[8] N. Bianchi, S. Bolognani, and M. Zigliotto, "High-performance PM synchronous motor drive for an electrical scooter," *IEEE Trans. Ind. Appl.*, vol. 37, no. 5, pp. 1348-1355, Sep/Oct 2001.

[9] B. H. Bea, N. Patel, S. Schulz, and S. K. Sul, "New field weakening technique for high saliency interior permanent magnet motor," *in Conf. Rec. IEEE IAS Annu. Meeting*, Oct. 2003, pp. 898-905.

[10] T. S. Kwon, G. Y. Choi, M. S. Kwak, and S. K. Sul, "Novel flux-weakening control of an IPMSM for quasi six-step operation," *IEEE Tran. Ind. Appl.*, vol. 44, no. 6, pp. 1722-1731, Nov./Dec. 2008.

[11] B. Cheng and T. R. Tesch, "Torque feedforward control technique for permanent-magnet synchronous motors," *IEEE Trans. Ind. Electron.*, vol. 57, no. 3, pp. 969-974, Mar. 2010.

[12] K. D. Hoang, Z.Q. Zhu, and M. Foster, "Online optimized stator flux reference approximation for maximum torque per ampere operation of interior permanent magnet machine drive under direct torque control," *in Proc. International Conf. Power Electron. Machine Drives, 2012,* Mar. 27- 29, 2012.

[13] D. G. Holmes and T. A. Lipo, *Pulse width modulation for power converters principle and practice*, New York: Willey-IEEE Press, 2003.

[14] R. Ottersten and J. Svensson, " Vector current controlled voltage source converter-deadbeat control and saturation strategies," *IEEE Trans. Power Electron.*, vol. 17, no. 2, pp. 279-285, Mar. 2002.

[15] K. M. Rahman and S. Hiti, "Identification of machine parameters of a synchronous machine," *IEEE Trans. Ind. Appl.*, vol. 41, no. 2, pp. 557-565, Mar./Apr. 2005.